CHARACTERIZATION OF FIBER WEAVE EFFECT ON HIGH SPEED PCBs

ONG YEE LUN

UNIVERSITI SAINS MALAYSIA

2015

CHARACTERIZATION OF FIBER WEAVE EFFECT ON HIGH SPEED PCBs

By

ONG YEE LUN

A Dissertation submitted for partial fulfilment of the requirement for the degree of Master of Science (Electronic System Design Engineering)

August 2015

ACKNOWLEDGEMENTS

Firstly, I would like to express sincere appreciations to my research advisor, Dr. Mohd Tafir Mustaffa, for his guidance and advice throughout my graduate study. His knowledge in the research field has helped me in addressing issues of the research topic.

This is followed by my advisor from Keysight Technologies, Mr. K.Y Lam, who gave me great technical insight, supports and consistent encouragements until the completion of this work. Besides that, I would like to thank Keysight ECAD Technical support team for providing helpful advice on the proper use of the CAD tool to avoid modeling geometry violation.

Lastly, I would like to express my gratitude towards my family members for their patience, support and encouragement throughout the research period.

TABLE OF CONTENTS

CHAPTER 2: LITERATURE REVIEW

CHAPTER 3: DESIGN METHODOLOGY AND CIRCUIT IMPLEMENTATION

CHAPTER 4: RESULTS AND DISCUSSIONS

LIST OF TABLE

LIST OF FIGURES

LIST OF ABBREVIATIONS

2D	2-Dimension
3D	3-Dimension
BER	Bit Error Rate
CILD	Controlled Impedance Line Designer
EM	Electromagnetic
FEM	Finite Element Method
Gbps	Giga Bits per Seconds
GHz	Giga Hertz
GT/s	Giga Transfers per Seconds
PCB	Printed Circuit Board
SSN	Simultaneous Switching Noise
TDR	Time Domain Reflectometry
TEM	Transverse Electromagnetic Wave
UI	Unit Interval

LIST OF SYMBOLS

Ω	Ohm
α	Attenuation Constant
β	Phase Constant
Ɛr	Relative Permittivity
γ	Propagation Constant
γ_p	Equivalent Propagation Constant
σ	Conductivity
C	Capacitance
G	Conductance
L	Inductance
R	Resistance
S	Second
V	Volt
Z	Characteristic Impedance
Z_p	Characteristic Impedance for Periodically Loaded Transmission Line

LIST OF APPENDICES

PENCIRIAN KESAN JALINAN SERAT PADA PAPAN LITAR CETAK KELAJUAN TINGGI

ABSTRAK

Trend mega pertumbuhan inovasi dan pembangunan telah membentuk era pengkomputeran lebih setengah abad dan masih diteruskan. Pensuisan isyarat elektrik hari ini memerlukan masa meningkat dan masa menurun dengan integrasi isyarat yang tinggi untuk memenuhi keperluan lebar jalur yang tinggi. Oleh itu, penghantaran isyarat antara pemancar dan penerima yang tahan lasak amat diperlukan kerana isyarat yang telah dihantar melalui saluran sistem akan mengalami herotan isyarat, degradasi terutamanya dalam penghantaran laluan yang panjang. Dalam kerja ini, metodologi pemodelan bagi papan litar cetak (PCB) telah dicadangkan termasuk kesan jalinan serat untuk mengkaji kesan serat pada isyarat bertentangan kutub kelajuan tinggi. Model simulasi 3-dimensi (3D) telah dibangunkan dengan perisian simulasi, Keysight Technologies EMPro untuk mencapai gambaran yang hampir dengan PCB komersil sebenar. Di samping itu, Keysight Technologies ADS simulator telah digunakan untuk menjalankan pencirian saluran dengan selanjutnya. Korelasi kajian antara 2-dimensi (2D) dan 3D EM model menunjukkan persamaan dengan teori. Hasil simulasi menunjukkan indeks kerataan yang tinggi seperti 1086-stail jalinan serat mengatasi prestasi kemampatan serat yang jarang seperti 1080 and 2113 dengan kehilangan sisipan yang rendah, gambarajah mata yang lebar dan tinggi, dan perbezaan masa yang rendah pada 0.44 ps seperti kajian kes 1. Selain itu, posisi wayar dengan tenunan serat yang tidak sejajar akan menyebabkan perbezaan masa tambahan pada 2.12 ps seperti yang dipaparkan dalam kajian kes 2. Akhirnya, kelebaran wayar dan jarak wayar ke wayar yang lebar seperti 6 / 10.9 mils terbukti mempunyai prestasi keseluruhan saluran yang

baik dalam kes 3 iaitu dengan menetapkan 100 Ω rintangan bertentangan sebagai pembolehubah tetap.

CHARACTERIZATION OF FIBER WEAVE EFFECT ON HIGH SPEED PCBs

ABSTRACT

The growth of innovation and development megatrend shaped the modern computing era for half a century and still counting. Today, switching signals are required to have faster rise and fall time with relative high signal integrity to meet higher digital signaling bandwidth. Therefore, it is very important to ensure reliable signal transmission link between the transmitter and receiver as the signal propagated through system channels will experience signal distortion, degradation especially in long haul transmission path. In this work, a methodology for printed circuit board (PCB) modeling is proposed which includes fiber weave fabrics to investigate the impact of fiber weave effect on high speed differential signaling. In order to achieve close representation of actual commercial PCB, 3-Dimension (3D) simulation models were developed through Keysight Technologies EMPro simulation software. Meanwhile, Keysight Technologies ADS simulator was deployed to further perform channel characterization. The correlation study between ideal 2-Dimension (2D) and 3D electromagnetic (EM) models showed good agreement with theory. The simulated results showed high flatness index spread glass weave such as 1086-style outperformed sparser weave like 1080 and 2113-style with lower insertion loss, wider eye width and eye height, and lowest timing skew at 0.44 ps in test case 1. Besides that, it is found that trace to weave position full misalignment induced extra timing skew at 2.12 ps in test case 2. Lastly, wider trace width and trace to trace separation at 6 / 10.9

mils is proven to have better overall channel performance at targeted 100 Ω differential impedance fixed variable set in test case 3.

CHAPTER 1

INTRODUCTION

This introduction chapter gives the background and the motivation behind to drive this research work. In addition, the objectives, scopes and contributions of this research will be covered in this chapter.

1.1 Research Background

Conventional methods of PCB channels testing and characterization started with good practice of rule of thumb during channel routing in layout phase. After the prototype board is fabricated, the board will undergo various tests to further characterize the channel performance. Under-performed channels will require engineers to revisit layout and fabrication phase by tackling board laminates materials, channel routing method or both. Therefore, this work is aimed to model the channel with readily available 3D EM simulator to study the unseen micro PCB effect, namely fiber weave effect. The simulation model is expected to bridge the gap between layout and fabrication phase by providing helpful insight on the simulated channel performance. Besides that, prototype board turn will be reduced to minimum as the prototype board is fabricated according to simulated channel model result. This will eliminate resources wastage and save prototyping cost indirectly with the aid of developed 3D EM simulation model.

1.2 Problem Statements

PCB and its compositional construction materials are the fundamental parts of system design in high speed backplane system (Yuesheng, Jinwen, Jun, Mingling, Baofeng, 2011). The construction of most PCB made up of fiberglass with resin-based dielectrics filled the interstitial gap. These two materials exhibit different electrical properties which can cause serious signal integrity degradation (Tong, Xu, Schutt, Cangellaris, 2014). Research by Scott and Chris (2005) supports laminates with irregular composite materials construction result local variation in relative dielectric constant, trace impedance and delay. Furthermore, differential signaling are prone to fiber weave variation which increases differential skew, signal dispersion and common mode conversion. Difference in propagation velocities between the 2 parallel differential traces can contribute to significant amount of timing skew accompanied by increased common mode voltage and degraded differential signal as illustrated in Figure 1.1 and 1.2 (Jeff, Richard, Xiaoning, 2007). Links which are sensitive to intra-pair skew due to the existence of fiber weave effect can lead to data transmission failures at high data transmission rates (Tong et al., 2014). Hence, board materials with lower loss tangents are needed to reduce abrupt signal attenuation caused by laminate loss (Yuesheng et al., 2011).

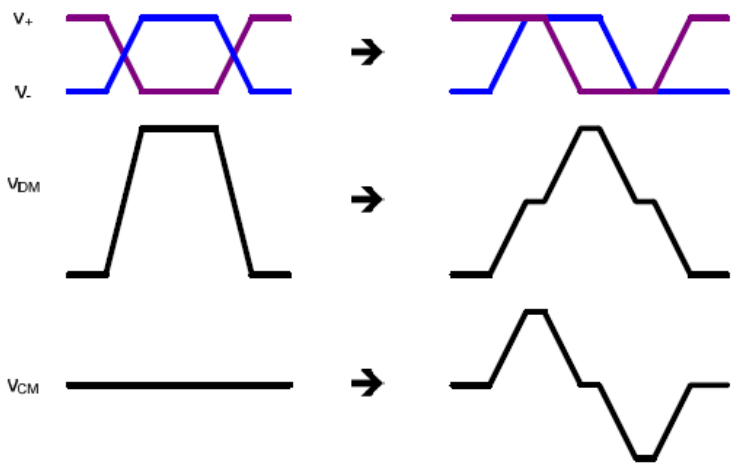

Figure 1.1: Skew effect on differential and common mode signal.

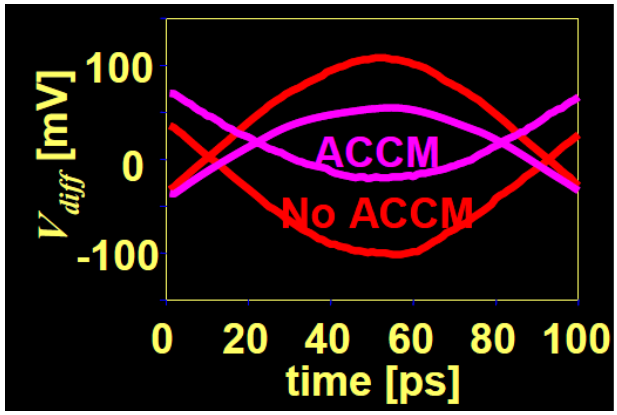

Figure 1.2: Skew effect on differential eye at 10Gb/s.

Therefore, denser fiberglass style would be preferred from homogeneity standpoint but the targeted cost and thickness of laminates imposed tradeoff between the two. Fiber weave effect simulation can be done based on the objective of the simulation, result accuracy and the simulation time taken (Gerardo, Chudy, Reydezel, Sueng-Won, Martin, 2011).

1.3 Research Objectives

This research work objectives are listed as followed:

(1) To characterize the presence of fiber weave effect on stripline differential signal transmission. Different types of fiber weave provide informative outcome on weave selection during pre-fabrication phase.

(2) To determine the best routing configuration to mitigate fiber weave effects. Strategic routing position provides the least fiber weave effect to differential signaling.

(3) To evaluate the channel performance over the intended operational frequency range.

1.4 Scope of Research

This research focuses on the modeling and characterization of PCB due to fiber weave effect. The simulation model are designed by using 1080, 1086 and 2113 weave types. The 3D model are compared and correlated back with simulated ideal 2D model results. The software used for modeling and circuit simulation are Keysight Technologies EMPro, 3D EM simulation software and Keysight Technologies ADS, an electronic design automation software for microwave, RF and high speed digital applications.

1.5 Research Contribution

This research contributes to the knowledge in high-speed channel design particularly in I/O signaling bandwidth for 8GT/s such as PCIe 3.0 and beyond. The design and development of the simulation model is anticipated to be one of the leading attempts in providing new trend of 3D full wave modeling and characterization of fiber weave effect to see the impact on induced timing skew and mode conversion which degraded the signal integrity of designed channel. This research contributes to knowledge in the following area of interests:

(1) Knowledge contribution in the R & D (Research and Development) of high-speed I / O (Input / Output) channel design by presenting simulation model which considers the effect of fiber weave rather than ideal channel model with bulk dielectric constant. Furthermore, comprehensive model analysis and performance discussion on different weave types, channel impedance, eye diagram, S-parameters and timing skew are presented.

(2) Presents the critical issues and challenges behind the design and development of the simulation model. As the transceiver I/O signaling speed is continuously increasing, a proper designed simulation methodology is needed to provide informative channel performance ahead. When these channels are fabricated for multi-gigabit signaling rates, PCB laminates no longer can be considered as homogeneous medium as different relative trace position with respect to weave will affect the signal integrity. Thus, relative routing position is demonstrated in this work to see the worst case scenario.

(3) Contribution to the knowledge in PCB fabrication industry by providing new methodology in the PCB stack-up construction planning. Therefore, this enables transmission channels specifically designed for particular high operating speed with the least effect due to fiber weaves type. As a result, trial and error characterization method will become a thing of the past. Other than that, significant amount of cost saving will be achieved as any under-performed designed channel will able to be screened before the board is sent for fabrication.

1.6 Thesis Organization

This thesis contains five chapters and is organized as followed:

Chapter 1 gives an introduction and the motivation behind this research. Besides that, this chapter also includes the research objectives and knowledge contribution to modern science and engineering.

Chapter 2 provides the overview of fiber weave effect, respective background knowledge and simulation methodology. Different types of simulation model construction and their pros and cons are discussed. This chapter also discusses techniques to mitigate fiber weave effects.

Chapter 3 discusses the design methodology and implementation of the proposed model. Moreover, various model configurations to characterize fiber weave effect on differential stripline is presented.

Chapter 4 includes the simulation results of the characterized models obtained from simulators. Detail analysis and discussion on the performance of the models are given. Also, a correlational study between the 3D model and the 2D ideal model are presented.

Chapter 5 concludes the findings of the work in this project. It also includes the future works that can be performed to further develop the research on fiber weave effect in PCB manufacturing industry.

CHAPTER 2

LITERATURE REVIEW

This chapter describes the necessary background knowledge required in order to have better understanding on this thesis work. Background knowledge of this work can be found from Chapter 2.1 to 2.7. Besides that, recent research efforts done by others are also presented in Chapter 2.8. Furthermore, the literatures on the modeling techniques used to characterize fiber weave effects are reviewed and compared against this work in Chapter 2.9. Lastly, the design recommendations and techniques to mitigate fiber weave effect are discussed in Chapter 2.10.

2.1 Fiberglass weave

Printed circuit boards (PCB) are constructed from woven bundles of fiberglass which has dielectric constant of approximately, 6 and glued together with epoxy resin of dielectric constant of 3.5 lead to non-homogenous dielectric medium for high speed digital signal propagation (Loyer et al., 2007). Fiber glass bundles come with different wrap and fill count, bundle thickness, spacing between two consecutive bundles in x and y-

direction, bundle pitch and etc. give rise to different glass styles as shown in figure 2.1. Typically, denser fiberglass style exhibits better homogeneity as the gap between 2 adjacent weave bundles is smaller (Luevano, Jaemin, Michalka, 2013).

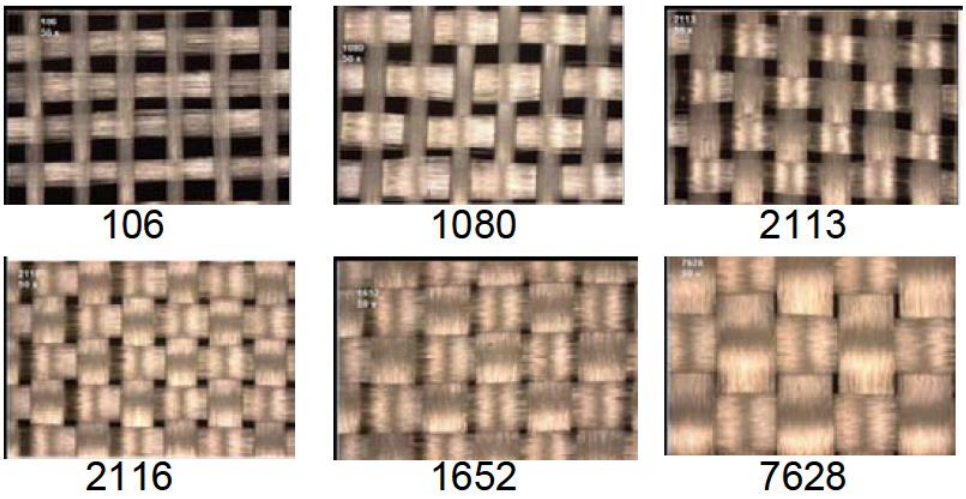

Figure 2.1: Various weave styles of fiber glass.

Properties of a laminate are determined by two additional micro-structural parameters due to lamination process are fibers' orientation with respect to loading direction and lamina's relative position with respect to adjacent laminae inside a lamina. There are three possible phase shift patterns identified, namely iso-phase, random-phase and out-of-phase as shown in figure 2.2. Iso-phase pattern is in-phase and has no change in phase shift relative to each lamina. Random-phase pattern has a phase shift between zero and ± 180°. Meanwhile, out-of-phase has a phase inversion of ±180°. The occurrences of phase shift under studies are due to error incurred due to stacking step and/or the laminae's movement during autoclave curing of the laminate (Gupta, Abhishek, Raghavan, 2011).

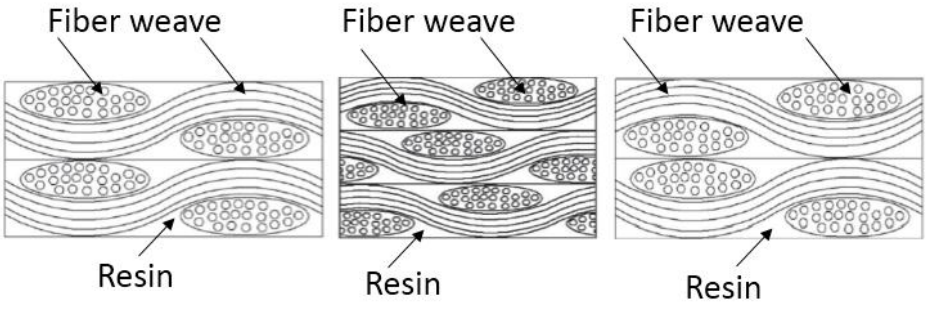

(a)Iso-phase. (b)Random-phase. (c) Out-of-phase.

Figure 2.2: Various phase shift patterns of laminae inside a woven laminate.

Next, the percentage of glass bundles and epoxy resin determine the nominal relative dielectric permittivity. V_{fiber} and V_{resin} are the dielectric volume ratio of epoxy resin and glass bundles while ε_{glass} and ε_{rsien} are the dielectric permittivies (Bucur, 2014).

$$\varepsilon_r = \varepsilon_{resin} V_{resin} + \varepsilon_{fiber} V_{fiber} \qquad \text{(Equation 2.1)}$$

Optimized glass weave manufacturing process to produce smaller interleaving pitch with low yet closer values between ε_{resin} and ε_{glass} such as spread glass is essential to ensure uniform glass weave distribution across glass fabric so that minimization of fiber weave effect is attainable. There are three types of fiberglass yarns such as E-glass, S-glass and NE-glass. E-glass, also known as electronic glass is widely used as strengthening fibers in the fiber glass fabrics. On the other hand, S-glass is often utilized for non-electrical applications. Meanwhile, higher-end laminates with better electrical and mechanical performance will employ NE-glass which exhibits lower dielectric permittivity, lower loss tangent, and lower Coefficient of Thermal Expansion (CTE) (Bucur, 2014). Lower cost PCB manufacturing for mass production can be achieved by adopting standard FR4 materials which made up of glass weaves bundles and resin. Thus, this provides an alternative to higher end products operated in millimeter wave region. Other than higher

performance yet expensive laminates such as PTFE, FR4 laminates with low dielectric constant and low loss are also suitable to be used in millimeter wave application. (Kaminski et al., 2013).

2.2 Differential Signaling

Differential signaling comprises a pair of positive and negative physical channels driven by the same amplitude but 180° out of phase polarity electrical signal (YueSheng et al., 2011). The advantage of differential signaling over single-ended data transmission is due to its effectiveness in common-mode noise rejection such as simultaneous switching noise (SSN), power or ground bounce noise and crosstalk provided the transmission traces are tightly coupled (Dong Gun, Heeseok, Seungyong, Bongcheol, Joungho, 2002). For example, the digital state of the single-ended waveform in Figure 2.3(a) no longer can be distinguished due to large common mode noise imposed on the trace pair. Single-ended signals are subtracted by a differential amplifier at the receiving end to recover the signals transmitted as shown in Figure 2.3(b) (Stephen & Howard, 2009).

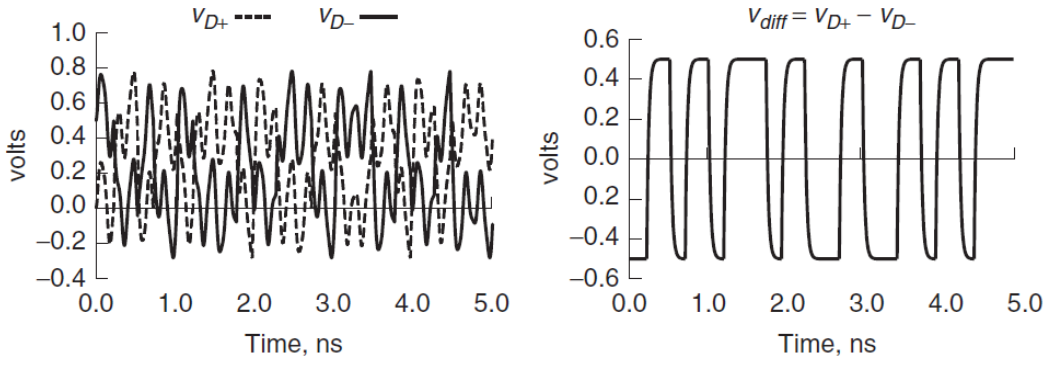

Figure 2.3(a, b): Single-ended waveforms at differential receiver with common mode noise, differential waveform after subtraction performed by differential amplifier.

2.3 Circuit Board Transmission Line

Two of the most generally used transmission line on PCB are microstrip and stripline. Microstrip can be further classified into non-buried Figure 2.4 (a) and buried Figure 2.4 (b). A microstrip has only one reference plane and is routed on outer layer of the PCB. Meanwhile, a buried microstrip is a trace which has only one reference plane but it is embedded inside dielectric such as solder mask. Apart from that, a stripline is embedded into the dielectric which sandwiched between two reference planes as shown in Figure 2.4(c) (Stephen & Howard, 2009).

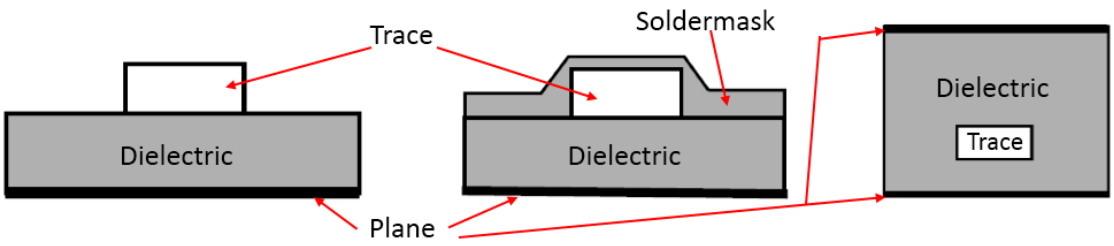

Figure 2.4: (a, b, c): Non-buried microstrip, buried microstrip, stripline (Left to right).

Characteristic impedance (Z_0) and per-unit length propagation delay (t_{pd}) of an ideal transmission line are real numbers and independent of frequency variation which can be expressed as followed:

$$Z_0 = \sqrt{\frac{L}{C}} \qquad \text{(Equation 2.2)}$$

$$t_{pd} = \sqrt{LC} \qquad \text{(Equation 2.3)}$$

where L and C are per unit length inductance and capacitance correspondingly. However, losses incurred on a realistic transmission line no longer can be ignored as the characteristic impedance becomes frequency dependent (Istvan Novak et al., 2013).

Therefore, a transmission line can be further represented as RLCG model in Figure 2.5 by employing a combination of series per unit length inductance (L) and resistance (R) with shunt per unit length capacitance (C) and conductance (G) (Kar et al., 2010).

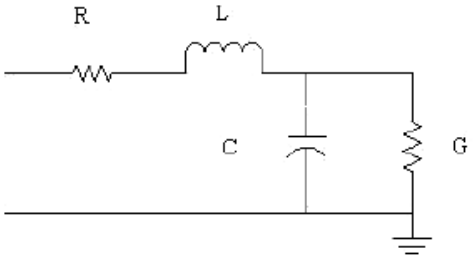

Figure 2.5: RLCG model for a segment of a transmission line.

The characteristic impedance of a lossy transmission line can be defined by Equation 2.4 with 4 R, L, C, G frequency dependent parameters. At the same time, the propagation constant (γ) which comprises of real and imaginary parts describe wave attenuation (α) and wave propagation (β) respectively as seen in Equation 2.5 (Istvan Novak et al., 2013).

$$Z_0 = \sqrt{\frac{R(f)+j\omega L(f)}{G(f)+j\omega C(f)}} \qquad \text{(Equation 2.4)}$$

$$\gamma(f) = \sqrt{[R(f)+j\omega L(f)][G(f)+j\omega C(f)]} = \alpha + j\beta(f) = \alpha + j\omega t_{pd} \qquad \text{(Equation 2.5)}$$

In addition, (Gustavo et al., 2011) presented attempts to obtain characteristic impedance by going through direct inversion method, renormalization, error model calculation, maximum identification and frequency adjustment. However, only two methods (maximum identification and frequency adjustment approaches) discovered produce

smoother line graph plots are utilized to further calculate RLCG parameters and followed by loss tangent (Gustavo et al., 2011).

2.3.1 Periodic Transmission Line

Furthermore, wave propagation along a transmission line embedded inside an alternatively repeating materials can be modelled as a transmission line with two discrete transmission line segments, namely 1 and 2 with R, L, C, G quantities as shown in the Figure 2.6 (Priya, Paul, Steve, 2013).

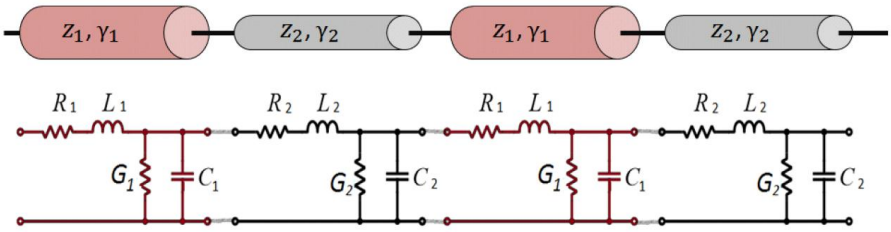

Figure 2.6: RLCG model for a two tone transmission line segment.

ABCD parameters for each arbitrary n^{th} tone of the transmission line cell unit with respective voltages and currents of "n" and "n-1" ports can be represented as:

$$\begin{bmatrix} V(n-1) \\ I(n-1) \end{bmatrix} = \begin{bmatrix} A & C \\ B & D \end{bmatrix} \begin{bmatrix} V(n) \\ I(n) \end{bmatrix} \qquad \text{(Equation 2.6)}$$

where A, B, C, D parameters are given by (Priya et al., 2013).

$$A = \cosh \gamma_1 l_1 \cosh \gamma_2 l_2 + \frac{Z(1)}{Z(2)} \sinh \gamma_1 l_1 \sinh \gamma_2 l_2 \qquad \text{(Equation 2.7)}$$

$$B = \cosh \gamma_1 l_1 \sinh \gamma_2 l_2 + Z_1 \sinh \gamma_1 l_1 \cosh \gamma_2 l_2 \qquad \text{(Equation 2.8)}$$

$$C = \frac{1}{Z(1)} \sinh \gamma_1 l_1 \cosh \gamma_2 l_2 + \frac{1}{Z(2)} \cosh \gamma_1 l_1 \sinh \gamma_2 l_2 \quad \text{(Equation 2.9)}$$

$$D = \cosh \gamma_1 l_1 \cosh \gamma_2 l_2 + \frac{Z(2)}{Z(1)} \sinh \gamma_1 l_1 \sinh \gamma_2 l_2 \quad \text{(Equation 2.10)}$$

A homogeneous line with minimum number of RLCG segments needed can be expressed as $n_{min} \approx \Delta.l.\beta$ where typical value of Δ is 4 for PCB technologies, l is the length of the line and β is propagation constant. The N number representation of periodic loads for a microstrip along the transmission line can be computed by using Equation 2.11 where l is the length of the transmission line, k is the unit cells length.

$$N = \frac{l}{k} \quad \text{(Equation 2.11)}$$

As a result, each unit cell constitutes **n** number of RLCG blocks where **n** can be expressed as in Equation 2.12.

$$n = \frac{n(min)}{N} \quad \text{(Equation 2.12)}$$

On the other hand, the number of blocks for stripline can be calculated by using Equation 2.13 and Equation 2.14 where N is different for top and bottom part of the transmission line. This is because of the load difference between the signal trace with respect to top plane and bottom plane (Romo et al., 2014).

$$N_{top} = \frac{n(min)}{N(top)} \quad \text{(Equation 2.13)}$$

$$N_{bottom} = \frac{n(min)}{N(bottom)} \quad \text{(Equation 2.14)}$$

2.4 Physical Structure of FR4 Laminate and Localized Dielectric Constant

One of the possible routing scene of the differential pair with the most significant routing is that one trace, D+ is routed over interleaved resin and fiber weave, whereas the other trace, D- is routed directly on top of the fiber glass bundle as seen in Figure 2.7(a, b). As a consequence, trace D+ will see a lower effective dielectric permittivity and higher impedance as compared to trace D- and vice versa (Stephen & Howard, 2009).

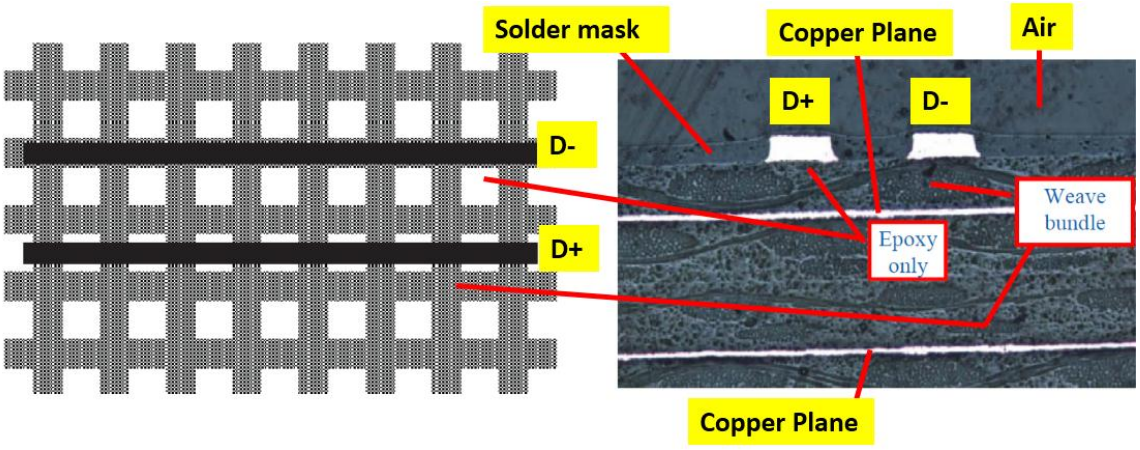

Figure 2.7(a, b): Top view of D+ and D- signal transmission line on a PCB, Cross-sectional view of D+ and D- microstrip.

2.5 Glass Weave Periodic Loading

Fundamental resonance frequency of glass weave can be predicted as a function of the material properties such as effective permittivity, pitch to pitch between glass weaves and also the angle between fiberglass weaves and the trace. Periodic loading leads to the occurrence of fundamental resonance at a particular frequency when half-wavelength equals to the separation distance between the periodic loads (Gerardo et al., 2011).

Associated resonance frequency (f_{res}) is given by:

$$f_{res} = \frac{c}{2\times\sqrt{\varepsilon eff\times pitch^2\times\left(\frac{1}{[\tan(\Phi)]^2}+1\right)}} \qquad \text{(Equation 2.15)}$$

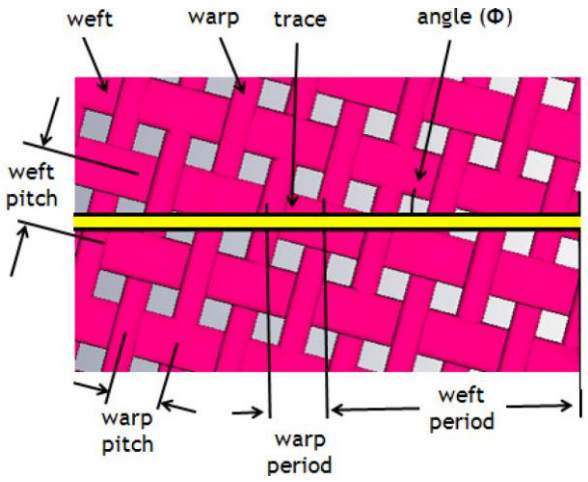

Figure 2.8: Terms defined for fiber weave effect analysis.

From Equation 2.15, c is the speed of light in vacuum, ε_{eff} is the effective permittivity of the dielectric, Φ is the angle between the trace and weft bundles while pitch is the "weft pitch" as seen from Figure 2.8. The Equation 2.15 applies to any arbitrary angle. When the angle Φ is greater than 45°, the weft and warp are swapped relatively with respect to the trace runs above. The weft and warp effects can be determined independently. For instance, the resonances induced would be out of frequency of interest for high speed interconnects due to the warp period seen is very small. As a result, warp induced loading effect due to very small period can be ruled out for now (Gerardo et al., 2011).

2.6 Floquet's Theorem

Floquet's theorem explains wave propagation phenomena in periodic media which must satisfy the condition whereby Equation 2.16. F (z) represents wave propagates in a periodic medium with periodicity in positive z direction while γ is the periodic propagation constant which describes the attenuation and propagation properties caused by the periodic structure.

$$F(z+p) = e^{-\gamma P} F(z) \qquad \text{(Equation 2.16)}$$

Electric field intensity of a wave propagate in z direction can be expressed as

$$E(x,z) = E(x)\, e^{-jBz} \qquad \text{(Equation 2.17)}$$

Equation 2.16 can be represented in Equation 2.17 in a periodic medium with L periodic pitch

$$E_k(x+L) = E_k(x) \qquad \text{(Equation 2.18)}$$

Application of Floquet's theorem on Equation 2.16 leads to Equation 2.19 where electric field intensity is dependent on K, "Bloch Wave Number". [Priya et al., 2011]

$$E(x,z) = E_k(x)\, e^{jKx} e^{jBz} \qquad \text{(Equation 2.19)}$$

Floquet's result can be applied to current and voltages in Equation 2.6 which is separated by period L at the ports of the two-tone periodic cell with Bloch Wave Number, K. Eigenvalue of the ABCD matrix is $e^{\pm jKL}$ in Equation 2.20.

$$\begin{bmatrix} A & B \\ C & D \end{bmatrix} \begin{bmatrix} V(2) \\ I(2) \end{bmatrix} = e^{\pm jKL} \begin{bmatrix} V(2) \\ I(2) \end{bmatrix} \qquad \text{(Equation 2.20)}$$

Dispersion relation is shown in Equation 2.21 where Bloch wave number can be conveyed as an inverse cosine function.

$$K = \frac{1}{L}\cos^{-1}\frac{A+D}{2} \qquad \text{(Equation 2.21)}$$

K is real when $\frac{1}{2}(A+D) \leq 1$ while K is imaginary and the wave is evanescent when $\frac{1}{2}(A+D) > 1$.

$$\frac{1}{2}(A+D) = 1 \qquad \text{(Equation 2.22)}$$

Forbidden Bands or Brillouin Zones define the boundaries where wave propagation due to periodic environment is evanescent as in Equation 2.22 with specified band edges and bandwidth. Besides that, normalized K and normalized ω are plotted in Figure 2.9 to show dispersion relation of an arbitrary selected periodic transmission line structure with the assumption of ideal transmission line in which R = G =0. Brillouin Zones are the shaded region when the imaginary value of K is non-zero. Several likely dispersion zones with unequal amplitudes and bandwidths in the range of frequency from 0 to 100GHz are observed (Priya et al., 2013).

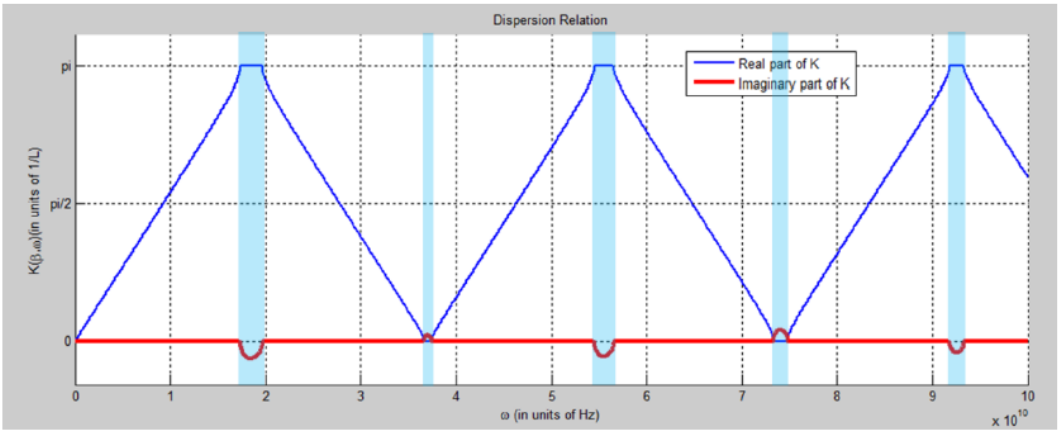

Figure 2.9: Dispersion Relation of a two tone periodic transmission line model.

2.7 Skew between two differential traces

Relative position is defined as an equally divided one weave pitch distance as shown in Figure 2.10.

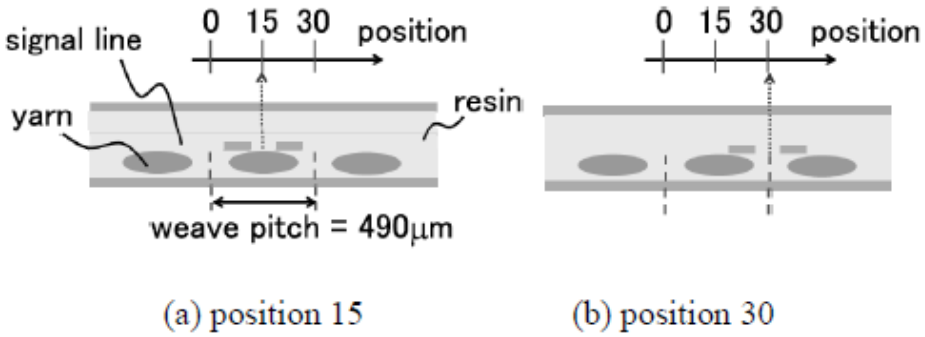

Figure 2.10: Relative position definition.

HFSS simulation results of a 2.5mm (98.43mil)-long transmission line shows small number of points where the skew values are about close to 0ps. Figure 2.7.1 shows a large number of skew values are hovering around 0.05 to 0.07 (maximum) and -0.05 to -0.07(minimum). The skew difference with respect to relative position obtained is approximated a 0.07 amplitude sinusoidal curve for the particular test case (Fukumori, Nagaoka, Mizutani, Tani, 2014).

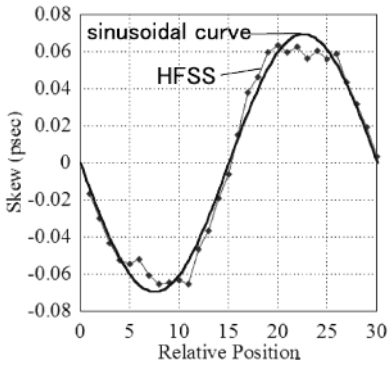

Figure 2.11: HFSS result plot and sinusoidal curve approximation.

In addition, the worst case skew observed for a 6 mil 6 inch differential signal is around 30 ps which is also 5ps/inch. Skew varies with offset due to different electric combination. Worst case skew for narrower trace reported at around 9ps/inch because of the asymmetric differential signaling (Kunz et al., 2014).

2.8 Modeling of Fiber Weave Effect

2.8.1 Statistical Analysis

Simulation models can be created as shown in Figure 2.12 where commercialized 2D extractors can solve the model with ease due to the geometry simplicity.

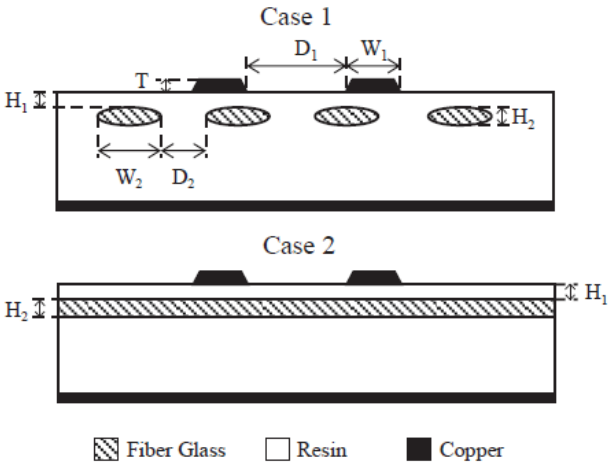

Figure 2.12: Simplified cross-sectional models to represent fiber weave effect.

Extraction of S-parameter matrices from 2D extractor is then imported to MATLAB and presented in the form of 4-port ABCD matrix for each unit section as outlined in Equation 2.6. The cascading property of ABCD parameters enables the use of matrix multiplication

to handle overall ABCD matrix if a long transmission line as in Equation 2.23 (Tong et al., 2014).

$$\begin{bmatrix} \mathrm{v}(1) \\ \mathrm{i}(1) \end{bmatrix} = \begin{bmatrix} A(1) & B(1) \\ C(1) & D(1) \end{bmatrix} \cdots \begin{bmatrix} A(m) & B(m) \\ C(m) & D(m) \end{bmatrix} \begin{bmatrix} \mathrm{v}(\mathrm{m}) \\ \mathrm{i}(\mathrm{m}) \end{bmatrix} \qquad \text{[Equation 2.23]}$$

Calculated S-parameter is imported to transient simulator to investigate intra-pair skew. Test circuit is driven by differential voltage sources with magnitude of 1.2V and 1GHz frequency as shown in Figure 2.13.

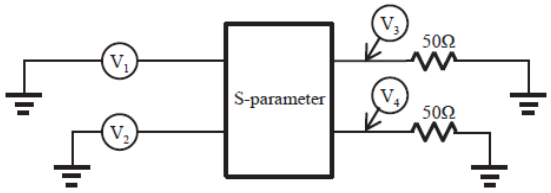

Figure 2.13 Test circuits for intra-pair skew measurement.

Monte Carlo analysis is performed and one million points sample space is taken to obtain probability distribution function of intra-pair skew. More than 20% of the samples simulated have very close intra-pair skew close to worst-case intra-pair skew of 8ps as seen in Table 2.1 (Tong et al., 2014).

Table 2.1: Intra-pair skew statistical data.

Percentage	Intra-pair Skew
10	> 8.30ps
20	> 8.03ps
30	> 7.50ps
40	> 6.78ps
50	> 5.91ps

This methodology incorporates the deployment of a 2D quasi-static EM solver, 2D extractor, MATLAB and a transient simulator to realize fiber weave model. The time-to-model development is shorten with increased efficiency as the geometry is not complicated to build as compared to 3D simulator. However, about 4 inch long differential microstrip line simulated in this paper is considered physically short to capture the timing skew at 1GHz. The impact of intra-pair skew at signaling frequency of 1GHz might not as profound as the differential transmission lines run at even higher frequency.

2.8.2 Perturbation Technique

Efficient modeling technique based on the solution of the relevant differential equations for non-uniform transmission line can be used to study the presence of fiber weave effect on transmission characteristics. Chain matrix approach is used as a reference to model 10 inches stripline pair as an alternating segment of a-b-a-b-… for 600 times to give rise 1200 chain matrix where the p.u.l parameters change in a piecewise constant number. The variation of the capacitance and inductance of the transmission line correspond to perturbation with and without mode coupling. The perturbation technique can apply to continuously varying p.u.l parameters with improved accuracy at very high frequencies by subdividing the longer line into shorter segments. Perturbation technique showed relatively high accuracy as compared to chain matrix technique shown in the graph plot of Figure 2.14. It can also be observed that the presence of fiber weave in PCB laminate contributes to insertion loss suck-out (Chernobryvko, Ginste, DE Zutter., 2013).

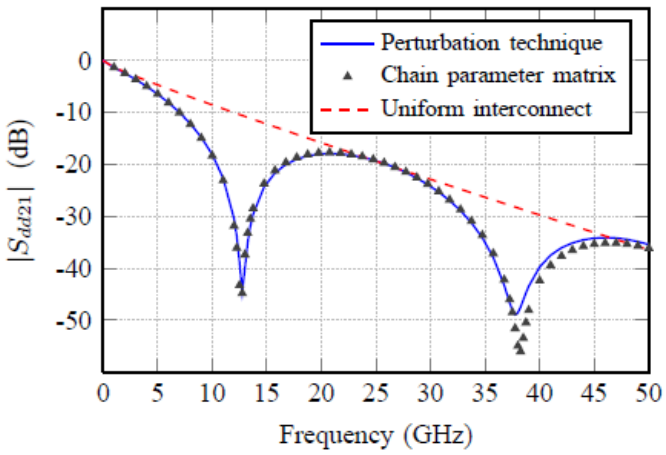

Figure 2.14: Insertion loss of various modelling techniques.

A 10” transmission line is modeled by varying the number of transmission line segments from 1 to 20 sections. The result showed substantial improvement for frequency span from 0 to 50GHz as seen in Figure 2.15. The computational time of the code consumed is heavily dependent on the number of “electrically short” transmission line section. The script ran in Matlab R209a shows significant improved efficiency with respect to standard chain matrix approach (Chernobryvko et al., 2013).

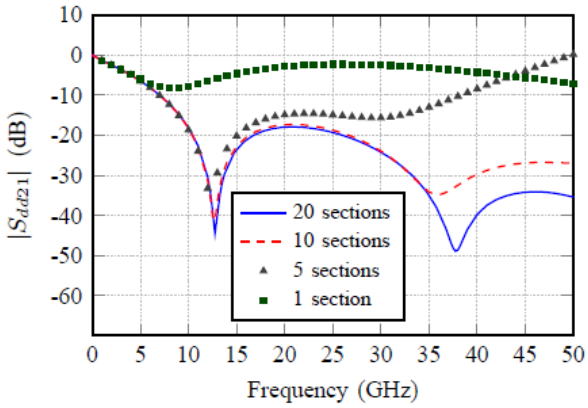

Figure 2.15: Insertion loss of the transmission line modelled with perturbation.